RESEARCH ARTICLE

WILEY

Increased segregation of structural brain networks underpins enhanced broad cognitive abilities of cognitive training

Quanjing Chen[1,2] | Timothy M. Baran[3,4] | Adam Turnbull[1,4] |
Zhengwu Zhang[5] | George W. Rebok[6] | Feng Vankee Lin[1,2,7,8,9]

[1]Elaine C. Hubbard Center for Nursing Research on Aging, School of Nursing, University of Rochester Medical Center, Rochester, New York

[2]Department of Psychiatry, School of Medicine and Dentistry, University of Rochester Medical Center, Rochester, New York

[3]Department of Biomedical Engineering, University of Rochester, Rochester, New York

[4]Department of Imaging Sciences, University of Rochester Medical Center, Rochester, New York

[5]Department of Biostatistics and Computational Biology, University of Rochester Medical Center, Rochester, New York

[6]Department of Mental Health, Johns Hopkins University, Baltimore, Maryland

[7]Department of Brain and Cognitive Sciences, University of Rochester, Rochester, New York

[8]Department of Neuroscience, School of Medicine and Dentistry, University of Rochester Medical Center, Rochester, New York

[9]Department of Neurology, School of Medicine and Dentistry, University of Rochester Medical Center, Rochester, New York

Correspondence
Quanjing Chen, and Feng Vankee Lin, CogT Lab, UR CABIN, 430 Elmwood Ave., Rochester, NY, 14620, USA.
Email: quanjing_chen@urmc.rochester.edu (Q. C.) and fengvankee_lin@urmc.rochester.edu (F. V. L.)

Abstract

A major challenge in the cognitive training field is inducing broad, far-transfer training effects. Thus far, little is known about the neural mechanisms underlying broad training effects. Here, we tested a set of competitive hypotheses regarding the role of brain integration versus segregation underlying the broad training effect. We retrospectively analyzed data from a randomized controlled trial comparing neurocognitive effects of vision-based speed of processing training (VSOP) and an active control consisting of mental leisure activities (MLA) in older adults with MCI. We classified a subset of participants in the VSOP as learners, who showed improvement in executive function and episodic memory. The other participants in the VSOP (i.e., VSOP non-learners) and a subset of participants in the MLA (i.e., MLA non-learners) served as controls. Structural brain networks were constructed from diffusion tensor imaging. Clustering coefficients (CCs) and characteristic path lengths were computed as measures of segregation and integration, respectively. Learners showed significantly greater global CCs after intervention than controls. Nodal CCs were selectively enhanced in cingulate cortex, parietal regions, striatum, and thalamus. Among VSOP learners, those with more severe baseline neurodegeneration had greater improvement in segregation after training. Our findings suggest broad training effects are related to enhanced segregation in selective brain networks, providing insight into cognitive training related neuroplasticity.

KEYWORDS
amnestic mild cognitive impairment, broad learning, cognitive intervention, DTI, graph theory

1 | INTRODUCTION

Induction of broad, far-transfer training effects is a major challenge in the field of cognitive training. This challenge is of particular importance: training games are most effective when they can be simply and repetitively administered, however, for them to have real-world impact they need to induce broad improvements in the multiple cognitive domains that underlie daily life challenges as a result of brain aging. Broad cognitive decline in executive function and episodic memory are particularly responsible for daily life difficulties in individuals with atypical brain aging, such as that arising due to Alzheimer's pathology. It is known that brain changes, especially structural changes, underpin cognitive changes from cognitive training (Lövdén, Backman, Lindenberger, Schaefer, & Schmiedek, 2010; Takeuchi et al., 2010). Thus far, studies related to brain structure have been focused on regional changes in grey matter. However, recent advances in cognitive neuroscience point to coherent systems of regions, or "networks", being the crucial units of complex brain function. Thus, studying the white matter connectome provides an opportunity to characterize neural circuits that potentially underpin multiple cognitive domains (Dai & He, 2014; Kraus et al., 2007). These circuits may represent the concerted engagement of latent components across multiple domains, and may provide information regarding the tasks that best engage these components. For example, targeting component processes that are fundamental in cognition, for example, process efficiency, may be particularly beneficial due to changes in neural circuitry that is flexibly engaged in a range of task, and therefore real-world, contexts (Lövdén et al., 2010).

For these changes to occur, individuals need to have the intrinsic or physiological capacity to adapt in response to training (Thayer, Hansen, Saus-Rose, & Johnsen, 2009). In dementia or the oldest old, when neurodegeneration exceeds the brain's capacity for plasticity (Park et al., 2004), such physiological adaptation can be minimal. Older adults at risk for dementia are among the most difficult group to induce broad training effects, accompanied with reduced white matter integrity (Fissler et al., 2017) and disrupted functional integrity (Liang, Wang, Yang, Jia, & Li, 2011). However, this group also represents a critical juncture for broad training effects to slow further cognitive deterioration. Therefore, understanding the mechanisms underlying broad training effects among older adults at risk for dementia, such as those with amnestic mild cognitive impairment (MCI), is a clinically and scientifically important research question. It is unclear if any brain regions are particularly relevant to broad, far-transfer training effects in MCI. Based on the literature on younger adults, the striatum is critical for transferring the effects of cognitive training across tasks sharing overlapping component processes (Dahlin, Neely, Larsson, Backman, & Nyberg, 2008). Alternatively, based on the cognitive aging literature, dorsolateral prefrontal cortex (DLPFC) is critical for providing compensatory support for different cognitive functions in aging: this mechanism may represent a natural capacity of the aging brain that improves functioning across multiple domains in response to neurodegeneration that could be enhanced by cognitive training (Park & Reuter-Lorenz, 2009). Regions involved in supporting specific cognitive functions may also play a role (e.g., hippocampus is involved in regulating long-term memory retrieval; frontal–parietal network is involved in regulating attention; Corbetta, 1998; Dudai, 2004; Goldman-Rakic, 1988). These systems are known to interact during complex tasks, and understanding whole-brain network-level changes is likely to be crucial for understanding broad training effects in both healthy and atypical aging populations.

Multiple studies have shown that the brain contains a number of functionally specialized networks, organized in a small-world topology to optimize efficiency of processing information (Bassett & Bullmore, 2009; Bullmore & Bassett, 2011; Bullmore & Sporns, 2009; Meunier, Lambiotte, Fornito, Ersche, & Bullmore, 2009). The nature of the small-worldness of a network is determined by two metrics derived from graph topology: a high clustering coefficient and short characteristic path length (Watts & Strogatz, 1998). The clustering coefficient quantifies the degree to which a cluster of nodes are fully connected to one another, while the characteristic path length describes the minimum distance between nodes. A high clustering coefficient reflects a high level of segregation between local clusters, indicating that information is being processed efficiently within localized brain networks. On the other hand, a short characteristic path length demonstrates integration between local clusters, indicating flexible communication of information across multiple local clusters (Boccaletti, Latora, Moreno, Chavez, & Hwang, 2006; Rubinov & Sporns, 2010). Both of these factors are essential in effective network functioning, and small-worldness relies on a balance between the two. Brain aging is known to cause changes in these metrics: it is often accompanied by reduced brain segregation due to neural dedifferentiation, and increased brain integration due to compensation via networks centered on DLPFC (Betzel et al., 2014; Chan, Park, Savalia, Petersen, & Wig, 2014; Geerligs, Renken, Saliasi, Maurits, & Lorist, 2015; Koen & Rugg, 2019; Onoda & Yamaguchi, 2013; Song et al., 2014). Reversing reduced segregation or enhancing compensation-integration are potential neural mechanisms underlying cognitive changes induced by interventions, particularly those that are likely to generalize across multiple domains and lead to real-world improvements (Bamidis et al., 2014; Cao et al., 2016; Langer, von Bastian, Wirz, Oberauer, & Jancke, 2013; Taya, Sun, Babiloni, Thakor, & Bezerianos, 2015). In line with this, increased segregation of brain functional networks was revealed in young adults after working memory training (Langer et al., 2013) and motor learning (Miraglia, Vecchio, & Rossini, 2018). Thus far, no study has examined the neural mechanisms underlying broad training effects following cognitive training in groups at risk of dementia by comparing segregation versus integration of brain networks. We suspect that strengthening of the brain's segregation, particularly in those local clusters regulating important fundamental cognitive components, would improve the broad training effect. Alternatively, brain integration may be enhanced, especially centered in the DLPFC that is known to play a role in compensation.

We recently completed a phase II double-blinded randomized controlled trial comparing the neurocognitive effects of vision-based speed of processing training (VSOP) and an active control consisting

of mental leisure activities (MLA) in older adults with MCI (Lin et al., 2020). VSOP trains processing speed and attention (PS/A), a cognitive domain essential to all cognitive operations (Salthouse, 1996; Woutersen et al., 2017). When comparing VSOP to MLA from baseline to immediately after intervention, there was a significant training effect on a PS/A measure that was not practiced in the VSOP training, as well as a selective transfer effect to working memory but no effect on episodic memory (Figure S1). In the present study, we retrospectively analyzed the intervention findings to identify a subset of participants with a broad far-transfer training effect (i.e., learner)—across executive function (EF, that is, working memory and cognitive control) and episodic memory (EM). Unfortunately, due to the small percentage of individuals showing broad learning following the active control (*n* = 5, see Figure 1a), the inclusion of a group consisting of MLA learners is impossible. For the purposes of this study, we therefore selected learners from the VSOP group only, with others in VSOP (i.e., VSOP non-learner) and non-learners in MLA as comparisons. In ideal circumstances, this study would be performed using four groups in a 2 (VSOP vs. MLA) by 2 (learners vs. non-learners) design. The lack of an actual comparison between two trainings (VSOP and MLA) in four groups (learners and non-learners for both VSOP and MLA) is therefore a major limitation of the study. Future work will be needed to test whether the broad training effect is specific to VSOP or can be generalized to other cognitive or lifestyle interventions.

We compared diffusion imaging based small-worldness indices between the VSOP learner and VSOP non-learner or MLA non-learner group; relevantly, a set of competitive hypotheses were tested surrounding integration versus segregation in relation to the broad training effect. Cumulative literature suggests the capacity to learn endures despite old age or neurodegeneration (Lampit, Hallock, & Valenzuela, 2014; Lövdén et al., 2010; Shao et al., 2015). Here, we investigated whether neurodegeneration at baseline affected the broad training effect. We computed neurodegeneration with Alzheimer's disease signature cortical thickness (ADSCT), with higher score indicating greater cortical thickness and lower severity in neurodegeneration. We tested whether the relationship between neurodegeneration at baseline and the neural enhancement differed in VSOP learner compared to non-learner.

2 | METHODS

2.1 | Overview of design

The protocol for the parent double-blinded randomized controlled trial is reported in NCT02559063, and the study CONSORT form is provided as Figure S2. Specific to the current study, we identified a subset of participants in the VSOP group who showed broad, clinically meaningful training effects across EF and EM (i.e., learner). The rest of the participants in the VSOP group (i.e., VSOP non-learner) served as the main group for comparison, with a subset of participants in the MLA group (i.e., MLA non-learner) acting as controls. Diffusion tensor imaging (DTI) was assessed at baseline and immediately after intervention to determine the brain structural networks associated with VSOP training's broad training effect. Furthermore, to test whether learners with altered networks were affected by neurodegeneration, we compared the relationship between baseline neurodegeneration
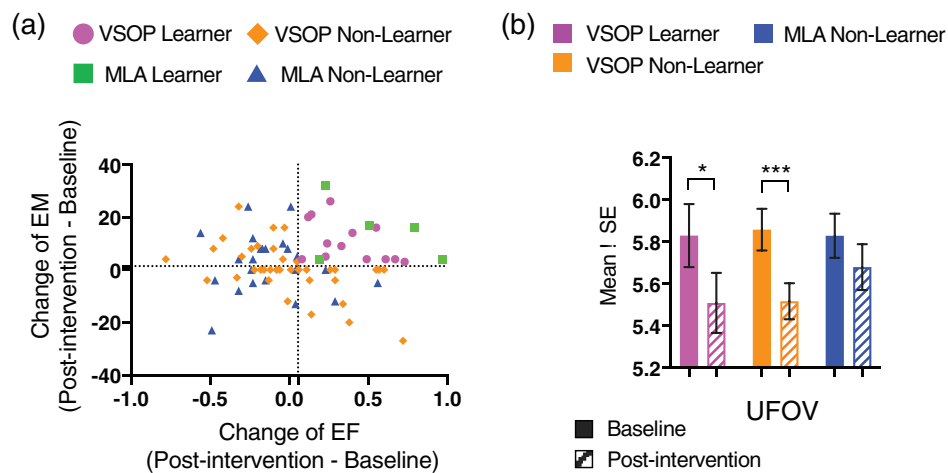

FIGURE 1 (a) Participant categorization. Participants were first randomized to VSOP versus MLA groups at 2:1 ratio. Participants were further assigned to either the learner or the non-learner group based on their performance on executive function and episodic memory at baseline and postintervention. Participants who achieved *clinically important differences*, that is, whose performance at postintervention assessment was higher than the baseline by at least one standard error of measurement, in both the executive function and episodic memory were classified as "learner", and the rest in VSOP and MLA groups were classified as "non-learner." The x-axis is the change of executive function from baseline to posttest. The y-axis is the change of episodic memory from baseline to posttest. The dotted line represents one standard error of the mean. (b) Baseline and postintervention performance in UFOV are plotted separately for VSOP learners (pink), VSOP non-learners (orange), and MLA non-learners (blue) groups. Error bars denote standard error of the mean. The asterisk represents significant within-group change from baseline. *$p < .05$; **$p < .01$; ***$p < .001$. UFOV, Useful Field of View (lower value indicates better performance)

and change of reveal networks after intervention between VSOP learners and non-learners. Of note, sustainability of the training effect is another topic not directly relevant to the current study; therefore, the 3- or 6-month follow-up data were not included in the paper.

2.2 | Participants

Eighty-four older adults with amnestic MCI (single- or multiple-domain) aged 60–90 years were recruited from University-affiliated memory, internal, and geriatric clinics. All clinics used 2011 diagnostic criteria for aMCI (Albert et al., 2011): (a) memory deficit (1–1.5 *SD* below age- and education-corrected population norms); (b) *may* have deficits in other cognitive domains (e.g., executive function); (c) preserved Basic Activities of Daily Life, defined as requiring occasional assistance on less than two items on the Minimum Data Set-Home Care interview; and (d) absence of dementia using NINCDS-ADRDA criteria. Other inclusion criteria included (a) if applicable, no change in dose of Alzheimer's medication (i.e., memantine or cholinesterase inhibitors) in the 3 months prior to recruitment; (b) capacity to give consent based on clinician assessment; and (c) other: age ≥60 years, English-speaking, adequate visual acuity for testing, and community-dwelling. Exclusion criteria included

(a) current enrollment in another cognitive improvement study; (b) uncontrollable major depression, or change of antipsychotic, antiseizure med, antidepressants or anxiolytics in the past 3 months; (c) MRI contraindications (e.g., pacemaker); (d) major vascular disease: stroke, myocardial infarction, or congestive heart failure. The study was approved by the University of Rochester Research Subject Review Board. Written consent was obtained from each participant. Since cognitive assessments vary across clinics, we reassessed memory (Brief Visuospatial Memory Test (Benedict, 1997), executive function (EXAMINER, Kramer et al., 2014), and global cognition (Montreal Cognitive Assessment, [Rossetti, Lacritz, Cullum, & Weiner, 2011]) at baseline. Subject characteristics are summarized in Table 1. We tested whether there were significant group differences in demographic characteristics or cognitive assessment tests at baseline.

2.3 | Intervention and group assignment

Participants were randomized to VSOP versus MLA groups at a 2:1 ratio. VSOP intervention was administered using a commercial package from Brain HQ, Posit Science, which included five computer games that target PS/A. All tasks share visual components, and the tasks become increasingly more difficult and require faster reaction

TABLE 1 Baseline characteristics

	VSOP learner (n = 12)	VSOP non-learner (n = 31)	MLA non-learner (n = 19)	T, F or χ² test, df1, df2, (P)
Age, mean (SD)	73.42 (7.93)	74.65 (7.37)	73.74 (6.10)	0.171, 2, 59 (.84)
Years of education, mean (SD)	16.54 (1.92)	15.85 (2.40)	16.84 (2.93)	1.00, 2, 59 (.38)
Male, n (%)	6 (50.0)	20 (64.5)	9 (47.4)	1.66, 2 (.43)
Non-hispanic White, n (%)	12 (100.0)[a]	28 (90.3)[a]	13 (68.4)[b]	**7.08, 2 (.03)**
Married, n (%)	9 (75.0)	25 (80.6)	14 (73.7)	0.38, 2 (.83)
GDS, mean (SD)	2.42 (1.93)	2.45 (2.42)	1.37 (1.61)	1.70, 2, 59 (.19)
Single-domain aMCI, n (%)	7 (58.3)	10 (32.3)	12 (63.2)	5.31, 2 (.07)
First-degree family history of AD, n (%)	7 (58.3)	15 (48.4)	9 (47.4)	0.42, 2 (.81)
Actively taking AD medication, n (%)	3 (25.0)	4 (12.9)	2(10.5)	1.37, 2 (.50)
BMI, mean (SD)	27.08 (4.24)	25.76 (4.37)	27.18 (5.00)	0.72, 2, 59 (.49)
Chronic condition index, mean (SD)	5.00 (2.73)	4.23 (2.01)	4.21 (2.49)	0.55, 2, 59 (.58)
• Hypertension, n (%)	6 (50.0)	14 (45.2)	13 (68.4)	2.62, 1 (.27)
• Diabetes, n (%)	2 (16.7)	4 (12.9)	0 (0.0)	3.08, 1 (.22)
Total minutes of training time, mean (SD)	1192.41 (325.82)[a]	1012.27 (467.99)[a]	1656.74 (408.34)[b]	**13.55, 2, 59 (<.001)**
MOCA, mean (SD)	24.25 (3.19)	23.94 (2.74)	24.89 (2.35)	0.07, 2, 59 (.93)
UFOV, mean (SD)	5.83 (0.52)	5.86 (0.54)	5.83 (0.46)	0.02, 2, 59 (.98)
EF, mean (SD)	−0.14 (0.45)	−0.11 (0.58)	0.07(0.47)	0.89, 2, 59 (.41)
EM, mean (SD)	38.50 (10.35)	38.71 (15.24)	39.26 (11.79)	0.67, 2, 59 (.51)
Neurodegeneration indexed by ADSCT, mean (SD)	2.82 (0.18)[a]	2.71 (0.15)[b]	2.76 (0.15)[a]	**3.90, 2, 59 (.026)**

Note: [a,b,c] represents the post-hoc comparison difference from the *F*-test. Bold values indicate *p* < .05.
Abbreviations: AD, Alzheimer's disease; ADSCT, Alzheimer's disease signature cortical thickness (for neurodegeneration); aMCI, amnestic mild cognitive impairment; BMI, body mass index; EF, executive function; EM, episodic memory; GDS, geriatric depression scale—15 items; MOCA, montreal cognitive assessment (for global cognition); UFOV, useful field of view.

times as training progresses (detailed description of the five PS/A tasks is provided in the *VSOP training tasks* section). Participants respond by identifying either the type or location of an object displayed on the screen. The training dynamically adjusts the difficulty of each task in real time based on the participant's performance, ensuring that the participant always operate near his/her optimal capacity. MLA intervention included online crossword, Sudoku, and solitaire games. Participants can choose to practice any combination of these games. The purpose is to control for computer and online experience and the amount of training time, and simulate everyday mental activities. For both groups, we provided identical online platforms, as well as orientation and two check-in sessions in-person. Participants completed all other training sessions at home. During the self-administration period, technical support was available by phone and email. The training period across both groups lasted 6 weeks, with participants instructed to complete four 1-hr sessions per week.

2.4 | VSOP training tasks

Briefly, a suite of five BrainHQ (Posit Science, CA) exercises that targeted PS/A was used for VSOP training. In Eye for Detail, a series of 3–5 images (e.g., butterflies) were briefly presented one at a time in different locations on the screen. Participants were required to identify the locations of the stimuli identical in appearance. Difficulty level changed as a function of the number of stimuli, as well as the contrast and distance between the stimuli. In Hawk Eye, a cluster of birds flashed briefly on the screen in peripheral vision. Participants were required to identify the location of the target bird that differed from the other distractor birds. Difficulty level varied in contrast between the birds and the background, stimulus duration, and diameter of the bird clusters. In Visual Sweeps, two sweep patterns (movement of bars) were presented simultaneously. Participants were required to determine whether each pattern moved inward or outward. Difficulty level changed as a function of color and luminance, orientation, and spatial frequency. In Double Decision, participants were required to identify which of two vehicle stimuli appeared in the center of the screen, as well as the location of a peripheral road sign. Difficulty level changed as a function of contrast between the center stimuli, number of peripheral stimuli, diameter of the field of view, and complexity of the background. In Target Tracker, a few target objects (e.g., bubbles) are displayed on the screen, followed by additional "distractors" identical in appearance. Participants were required to track the target objects as all of the objects moved in Brownian motion, then select the targets after the stimuli stopped moving. Difficulty level varied in number of target objects, speed and duration of object motion, and contrast between the objects and the background. All tasks shared visual components, and the tasks became increasingly more difficult as subjects' training progressed, thus requiring faster reaction times. Responses were based on object type or location and orientation on the screen. The training automatically adjusted the difficulty of each task based on each participant's performance, ensuring that participants always trained near their maximum capacity on each task.

2.5 | Outcome assessments and definition of clinically important improvement

To evaluate the intervention trained effect, we measured PS/A using Useful Field of View (UFOV), a three-task computer test that assesses processing speed, sustained attention, and divided attention based on reaction time. A composite score was created by averaging the reaction times of the three tasks, with higher scores indicating slower reaction time and poorer performance. Then the composite score was log transformed to account for a heavily right-skewed distribution. The tasks in UFOV were conceptually identical to VSOP training but in different formats.

For the VSOP group, participants were further assigned to either the learner or the non-learner group based on their change of performance on EF and EM from baseline to postintervention. EF was measured using EXAMINER (Kramer et al., 2014), a computerized test designed for clinical trials that measures executive function. A composite score was generated by averaging the composite scores from two executive function domains: cognitive control (set shifting and flanker tasks) and working memory (dot counting and 1-back). EM was measured using the Brief Visuospatial Memory Test (BVMT-R); Benedict, 1997). A composite score was developed by averaging the T scores from learning and delayed recall. It is worth noting that we purposely used visual stimuli for the cognitive tests, since previous literature indicated that transfer effects may be restricted to domains sharing a latent structure (in this case, visual attention; Lövdén et al., 2010). Participants who achieved *clinically important improvement*—the composite score for performance at postintervention was higher than the baseline by at least one standard error of measurement (Copay, Subach, Glassman, Polly Jr., & Schuler, 2007)—in both EF and EM were classified as "learner," and the rest in VSOP group were classified as "non-learner." We excluded seven participants who dropped out of the study during the intervention period (refer to CONSORT form, Figure S2). In addition, non-learners in MLA group served as a control. The categorization is displayed in Figure 1a. Of note, we did not use the Montreal Cognitive Assessment (MOCA) to reflect a broad training effect since it is considered a screening tool (Rossetti et al., 2011).

We also tested group differences in postintervention performance of UFOV using ANCOVA with group (VSOP learner vs. VSOP non-learner vs. MLA non-learner) as a fixed factor and baseline performance, neurodegeneration, and total amount of training time as covariates. The change from baseline to postintervention within each group was tested with paired t-tests.

2.6 | Brain structural network data collection, preprocessing, and analysis

2.6.1 | Imaging data acquisition and preprocessing

Imaging data were collected at University of Rochester Center for Advanced Brain Imaging and Neurophysiology (UR CABIN), using a

3 T Siemens TrioTim scanner (Erlangen, Germany) equipped with a 32-channel head coil. *Structural MRI*: high-resolution T1-weighted anatomical images were collected with TR/TE = 2,530 ms/3.44 ms, TI = 1,100 ms, flip angle = 7°, 256 × 256 matrix, 1 mm³ isotropic resolution, 1 mm slice thickness, and 192 slices. *Diffusion MRI*: DTI was performed using a 2D axial single-short dual-echo SE-EPI sequence with TE/TR = 86 ms/8900 ms, 128 × 128 matrix, 2 mm slice thickness with no gap (60 slices for whole brain coverage), iPAT (GRAPPA) acceleration factor = 2, 60 diffusion-weighted directions with b = 1,000 sec/mm² and 1 average, and b = 0 images with 10 averages. Each raw diffusion weighted imaging (DWI) image was aligned to the average b0 image using the FSL eddy correct tool (www.fmrib.ox.ac.uk/fsl) to correct for head motion and eddy current distortions. Non-brain tissue was removed using FSL's Brain Extraction Tool (Smith, 2002). We then registered DWI images with the T1 anatomical images using Advanced Normalization Tools (ANTS; http://www.picsl.upenn.edu/ANTS/).

2.6.2 | Network construction

To extract brain connectome, we employed an established structural connectome processing pipeline (for details see Zhang et al., 2018). First, we applied a reproducible probabilistic tractography algorithm (Girard, Whittingstall, Deriche, & Descoteaux, 2014) to diffusion MRI data to generate streamlines across the whole brain. Next, we defined the cortical, subcortical and brainstem regions on T1 anatomical images for each participant using FreeSurfer (http://surfer.nmr.mgh.harvard.edu/). From the FreeSurfer segmentation, 17 subcortical, and brainstem structures were identified: the brain stem, and bilateral segmentations of thalamus, caudate, putamen, pallidum, hippocampus, amygdala, accumbens, and cerebellum. Automated cortical parcellation was identified using the Desikan–Killiany Atlas including 34 regions per hemisphere (Desikan et al., 2006). Together, we obtained 85 nodes per participant. For each pair of nodes, we extracted the streamlines connecting them. Next, we calculated the mean fractional anisotropy (FA), an indicator of myelination and axonal thickness, from the streamlines to describe the connectivity (edge) between the connected nodes. Of note, we focused on FA since it produces reliable graph measures with high precision (Yuan et al., 2019). This whole procedure generated an 85-by-85 symmetric FA-based weighted structural connectivity matrix per participant at baseline and postintervention, respectively.

2.6.3 | Graph theoretical analysis

We investigated the topologic properties of brain networks at both the global and nodal level with the GRETNA toolbox (Wang et al., 2015). Two metrics for quantifying the small-worldness were used, clustering coefficient and characteristic path length.

The clustering coefficient, a measure of the degree to which nodes in a graph tend to cluster together, reflects the network

segregation in the brain. A larger clustering coefficient represents greater segregation. For each node, this can be calculated as the proportion of connections between the nodes within its neighborhood divided by the number of all possible connections between them. The neighborhood for a node is defined as its immediately connected nodes:

$$C_i = \frac{t_i}{k_{g_i}(k_{g_i} - 1)/2}$$

where g_i is the subgraph that contains the direct neighbors of node i, t_i is the total number of connections in g_i, k_{g_i} is the number of nodes in g_i, and $k_{g_i}(k_{g_i} - 1)/2$ is the total number of all possible connections in g_i.

At the global level, the nodal clustering coefficients of all nodes can be averaged into the mean clustering coefficient:

$$C_{global} = \frac{\sum_{i=1}^{N} C_i}{N}$$

where N is the total number of nodes in the brain.

The characteristic path length, which is the average shortest distance between two nodes, indicates the network integration in the brain. A smaller characteristic length represents greater integration. At the nodal level, this can be calculated as the average shortest path length between a node and all other nodes:

$$L_i = \frac{\sum_{j=1, j \neq i}^{N} L_{i,j}}{N - 1}$$

where the minimum path length $L_{i,j}$ between a node i and node j is the minimum number of connections that needs to be traveled to go from a node i to node j.

At the global level, the characteristic path length the average of shortest path length over all nodes:

$$L_{global} = \frac{\sum_{i=1}^{N} L_i}{N}$$

These two metrics, clustering coefficient and characteristic path length, form the basis of many graph theoretical investigations (Bullmore & Sporns, 2009). Small-worldness is calculated as the ratio of clustering coefficient to characteristic path length by comparing to random graphs. A network can be said "smallworld" if its small-worldness is greater than one (Humphries & Gurney, 2008).

The resulting symmetric FA-based matrices were converted to graphs by applying a threshold. Because there is no definitive way to select a single threshold, we applied a fixed density threshold (defined as the total number of edges in a network divided by the maximum possible number of edges) in a range between 35 and 50% at intervals of 1% for each connectivity matrix. This range was chosen to ensure that 90% of the nodes were connected and small-worldness was <1 (Achard & Bullmore, 2007; He, Chen, & Evans, 2008). We calculated

both the global and nodal network topology metrics at each density. We further obtained a summarized score by computing the area under the curve (AUC) over the density threshold range for each network metric. The integrated AUC has been applied in previous studies of graph theoretical analysis of brain networks (Cao et al., 2013; Gong et al., 2009). The obtained integrated AUC values were used for further statistical analysis. To test the reliability of graph theory measures, we calculated the correlation between the baseline and postintervention global metrics for the MLA group. Graph theory metrics showed very good reliability (Pearson r = .646, p < .001 for global clustering coefficient; Pearson r = .935, p < .001 for characteristic path length).

2.6.4 | Statistical analyses

All statistical analyses were performed using SPSS version 24.0 (IBM). The normality of graph theory indices was assessed using the Kolmogorov–Smirnov test and parametric tests were performed when the data satisfied normal distribution. We tested between-group differences in postintervention outcomes with ANCOVA and compared baseline and postintervention results within each group using paired t-tests. The Levene-test was performed to assess the equality of variances for ANCOVA. The effect size with 95% confidence intervals (CI) was calculated for main effect of group with ANCOVA using partial-η^2 (η_p^2), with $\eta_p^2 \geq .01$ indicating a small, ≥.06 a medium, and ≥.14 a large effect. For paired comparisons (baseline vs. postinterventions), the effect size with 95% CI was calculated using Hedges'g index (similar to the Cohen's d statistic, with values ≤0.20 considered small, values around 0.50 considered medium, and values about 0.80 considered large.

Global level network analysis
We examined the group difference in global level network topology metrics. Postintervention network metric was entered as the dependent variable in an ANCOVA with group (VSOP learner vs. VSOP non-learner vs. MLA non-learner) as a fixed factor and baseline network metric, neurodegeneration, and total amount of training time as covariates. Planned contrasts were conducted to compare the VSOP learner group with the other two groups. Within each group we compared baseline with postintervention with paired t tests.

Nodal level network analysis
We further investigated at the nodal level to localize specific brain regions for which the network metric was altered differently across groups. For each node, the postintervention network metric was entered as the dependent variable in an ANCOVA with group (VSOP learner vs. VSOP non-learner vs. MLA non-learner) as a fixed factor and baseline network metric, neurodegeneration, and total amount of training time as covariates. A false discovery rate (FDR) procedure was performed at a p value of 0.01 to correct for multiple comparisons across 85 regions. Planned contrasts were conducted to compare the VSOP learner group with the other two groups. For significant

brain regions, we examined within-group differences between baseline and postintervention with paired t tests.

Neurodegeneration analysis
Neurodegeneration was quantified using structural MRI data by calculation of Alzheimer's disease signature cortical thickness (ADSCT), consisting of posterior brain regions, including bilateral inferior and middle temporal lobes, entorhinal cortex, and fusiform gyrus, based on automated cortical parcellation using the Desikan–Killiany Atlas with Freesurfer (Jack Jr. et al., 2015; Lin et al., 2017). Higher values in Alzheimer's disease signature cortical thickness indicate greater cortical thickness and lower severity in neurodegeneration.

We averaged the nodal network metric across the brain regions found to be significant (as described above), and tested whether the association between baseline ADSCT and post intervention averaged nodal network metric differed between VSOP learners versus non-learners using a generalized linear model, while controlling for the main effects of baseline ADSCT, Group (taking VSOP non-learner as the reference) and baseline averaged nodal network metric (y *Postintervention averaged nodal network metric* = $\beta_0 + \beta_1$ *Baseline averaged nodal network metric* + β_2 *Group* + $\beta_{3Baseline\ ADSCT}$ + β_4 *Baseline ADSCT* × *Group* + ε). We also included neurodegeneration as a covariate when comparing the between-group network topological properties.

3 | RESULTS

Seven subjects dropped out during the intervention period and ten were excluded due to inadequate tractography quality in either baseline or postintervention. In summary, there were 12 VSOP learners, 31 VSOP non-learners, and 19 MLA non-learners.

3.1 | Baseline difference in sample characteristics

Group comparison of baseline characteristics is presented in Table 1. The three groups did not differ significantly in demographic characteristics or cognitive assessment tests at baseline except for the race (p = .03). Significant group differences in total amount of training time were found (p < .001); the MLA non-learner group showed longer training time than the VSOP groups (p < .05), but no difference between VSOP learner versus VSOP non-learner. VSOP learner and MLA non-learner group showed less severe aging-associated neurodegeneration (indexed by higher ADSCT values) than VSOP non-learner at baseline (p < .05).

3.2 | Cognitive outcomes

We tested group differences in postintervention performance of UFOV with group (VSOP learner vs. VSOP non-learner vs. MLA non-learner) as a fixed factor and baseline performance, neurodegeneration, and

total amount of training time as covariates. There was a significant group effect in UFOV ($F[2,55] = 3.59$, $p = .034$). Post-hoc analyses revealed that compared to VSOP non-learners, VSOP learners had similar postintervention performance in UFOV ($p = .614$), and MLA non-learners showed worse postintervention performance in UFOV ($p = .026$). For within-group change, there was significant improvement in UFOV in VSOP learners ($t[11] = −2.85$, $p = .016$) and VSOP non-learners ($t[29] = −6.09$, $p < .001$), but not in MLA non-learner ($t[18] = −1.86$, $p = .079$; Figure 1b).

3.3 | Network analysis results

Both the global clustering coefficients and characteristic path length followed the normal distribution with Kolmogorov–Smirnov test p values >.05. Figure 2a shows histograms of global metrics at baseline, with normal distribution overlaid. All the ANCOVA tests across global and nodal level analysis meet the assumption of homogeneity of variance ($p > .05$).

For between-group comparisons in postintervention global clustering coefficient, controlling for baseline global clustering coefficient, neurodegeneration and total amount of training time, there was a significant group effect after intervention ($F(2,56) = 7.58$, $p = .001$, $\eta_p^2 = .213$, 95% CI [.040, .364]). Planned contrasts showed VSOP

learners had greater global clustering coefficient after intervention, compared with VSOP non-learners ($p = .025$) and MLA non-learners ($p < .001$). For within-group change of the global clustering coefficient, VSOP learners had a significant increase from baseline to postintervention ($t(11) = 3.46$, $p = .005$, Hedges' g = .591, 95% CI [.181, 1.073], see Figure 2b, left). No significant change was found for the other groups. This result suggests that individuals that showed a broad training effect following training showed a significant increase in whole-brain segregation that was not present in individuals not showing this effect.

To identify whether these changes were predominantly driven by any specific brain regions within the whole-brain network, we conducted a nodal-level analysis. Controlling for baseline nodal clustering coefficient, neurodegeneration and total amount of training time, there was a significant group effect for postintervention nodal clustering coefficient in the right caudal ACC (anterior cingulate cortex), right supramarginal gyrus, left postcentral gyrus, left putamen, and left thalamus (all p's < .01 with FDR correction and with large effect sizes of $\eta_p^2 = .179–.283$, see Table 2). Planned contrasts showed that VSOP learners had greater postintervention nodal clustering coefficients, compared with VSOP non-learners and MLA non-learners in all five regions (all p's < .01). Paired t tests showed that VSOP learners had significant increased nodal clustering coefficient from baseline to postintervention in all five regions with medium-to-large effect sizes

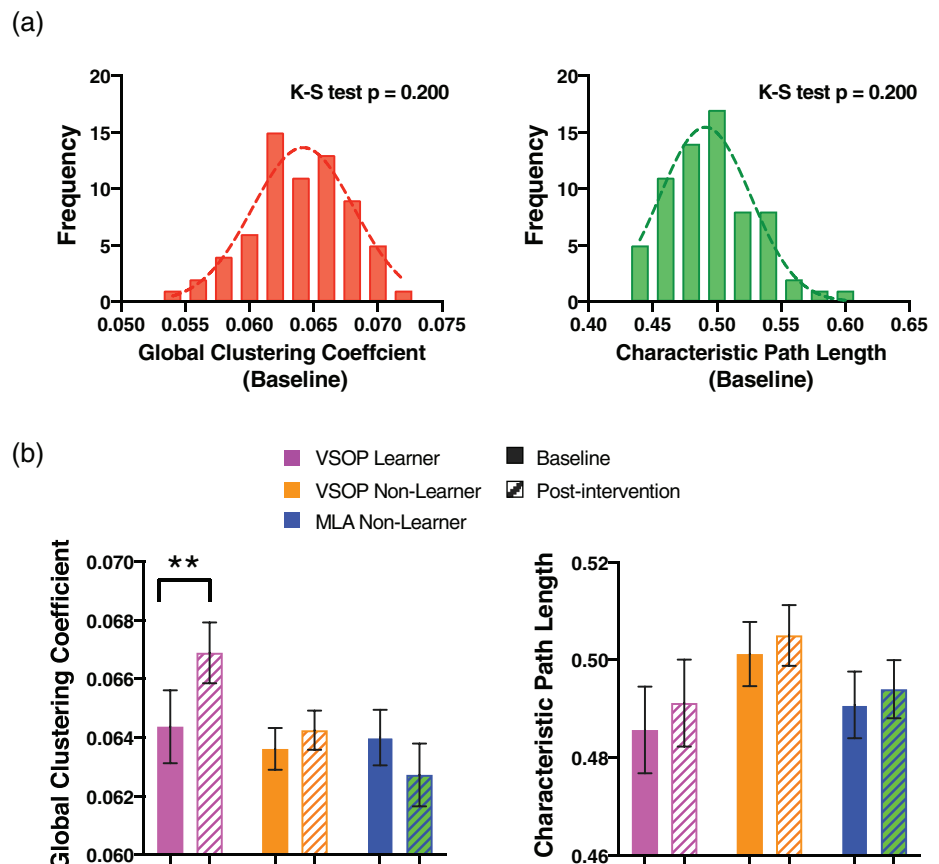## Global topology metrics

(a)

(b)

FIGURE 2 (a) Histograms of global small-worldness topology metrics at baseline, overlaid with bell-shaped curve. K–S test, Kolmogorov–Smirnov test. (b) Change of global small-worldness topology metrics from baseline to postintervention for VSOP learners (pink), VSOP non-learners (orange), and MLA non-learners (blue) groups. Error bars denote standard error of the mean. Star represents significant within-group change from baseline to postintervention. *$p < .05$; **$p < .01$; ***$p < .001$

TABLE 2 Brain regions with significant group effects in nodal clustering coefficient after FDR correction

Brain regions	VSOP learner (N = 12)		VSOP non-learner (n = 31)		MLA non-learner (n = 19)		ANCOVA on postintervention nodal metric, controlling for baseline nodal metric, neurodegeneration and total amount of training time	Planned contrasts	
	Baseline M (SD)	Posttest M (SD)	Baseline M (SD)	Posttest M (SD)	Baseline M (SD)	Posttest M (SD)	Effect of group	VSOP learner vs. VSOP non-learner	VSOP learner vs. MLA non-learner
R-Caudal ACC	0.067 (0.007)	0.073 (0.008)	0.067 (0.006)	0.066 (0.006)	0.066 (0.006)	0.065 (0.007)	$F_{(2,56)} = 11.07$, $p < .001$, $\eta_p^2 = .283$, 95% CI [.090, .435]	$p < .001$	$p = .003$
R-Supramarginal gyrus	0.068 (0.006)	0.074 (0.006)	0.070 (0.006)	0.070 (0.006)	0.071 (0.004)	0.068 (0.005)	$F_{(2,56)} = 9.47$, $p < .001$, $\eta_p^2 = .253$, 95% CI [.066, .407]	$p = .001$	$p < .001$
L-Postcentral gyrus	0.071 (0.008)	0.075 (0.007)	0.072 (0.008)	0.070 (0.007)	0.070 (0.007)	0.068 (0.006)	$F_{(2,56)} = 7.00$, $p = .002$, $\eta_p^2 = .200$, 95% CI [.033, .360]	$p = .001$	$p = .002$
L-Putamen	0.053 (0.004)	0.056 (0.004)	0.053 (0.005)	0.053 (0.004)	0.054 (0.005)	0.052 (0.005)	$F_{(2,56)} = 6.10$, $p = .004$, $\eta_p^2 = .179$, 95% CI [.022, .333]	$p = .007$	$P = .002$
L-Thalamus	0.053 (0.004)	0.056 (0.004)	0.054 (0.004)	0.054 (0.003)	0.055 (0.004)	0.053 (0.004)	$F_{(2,56)} = 7.46$, $p = .002$, $\eta_p^2 = .210$, 95% CI [.039, .366]	$p = .006$	$p < .001$

$t_{(11)} = 2.95$, $p = .013$, Hedges' g = .807, 95% CI [.175, 1.531] for right ACC; $t_{(11)} = 4.12$, $p = .002$, Hedges' g = .859, 95% CI [.306, 1.530] for right supramarginal gyrus; $t_{(11)} = 2.68$, $p = .022$, Hedges' g = .616, 95% CI [.069, 1.241] for left postcentral gyrus; $t_{(11)} = 2.66$, $p = .022$, Hedges' g = .631, 95% CI [.067, 1.275] for left putamen; $t_{(11)} = 3.68$, $p = .004$, Hedges' g = .607, 95% CI [.185, 1.111] for left thalamus). These findings suggest that, in addition to whole-brain increase in segregation, broad training corresponds with increased segregation of both cortical and subcortical nodes. MLA non-learners had significant decreased nodal clustering coefficient from baseline to postintervention in the right supramarginal gyrus ($t_{(18)} = -2.80$, $p = .012$, Hedges' g = −.635, 95% CI [−1.182, −.012]), left putamen ($t_{(18)} = -2.39$, $p = .028$, Hedges' g = −.383, 95% CI [−.747, −.043]) and left thalamus ($t_{(18)} = -2.52$, $p = .021$, Hedges' g = −.479, 95% CI [−.912, −.076]). The results are presented in Figure 3.

For characteristic path length, there were no significant between- or within-group differences at global level (see Figure 2b, right). No significant group differences were found at nodal level after FDR correction. This suggests that, in contrast to differences identified in network segregation, integration did not change significantly in individuals characterized by broad training improvements.

3.4 | Relationship between revealed networks and neurodegeneration

We averaged the nodal clustering coefficient across the five regions and tested whether the relationship between neurodegeneration at baseline and the neural enhancement differed between VSOP learner versus VSOP non-learner. There was a significantly stronger association between lower ADSCT and greater increase in postintervention averaged nodal clustering coefficient in learners than non-learners (B = −0.011, SE = 0.006, Wald's χ^2 = 4.39, $p = .036$), controlling for the main effect of ADSCT, group and baseline averaged nodal clustering coefficient. Post-hoc analysis revealed a significant negative relationship between ADSCT and postintervention averaged nodal clustering coefficient in learners (Pearson r = −.62, $p = .042$, 95% CI [−0.880, −0.072]), but no relationship in VSOP non-learners (Pearson r = −.03, $p = .860$, 95% CI [−0.380, 0.328]), controlling for baseline averaged nodal clustering coefficient (see Figure 4). This suggests that within individuals who demonstrate a broad learning effect, participants with greater neurodegeneration show the greatest increase in segregation within these brain regions.

4 | DISCUSSION

The results of this study reveal that enhanced segregation in DTI-based brain topology may be associated with broad training effects following cognitive training using PS/A in older adults with MCI. Particularly, right caudal ACC, right supramarginal gyrus, left postcentral gyrus, left putamen, and left thalamus were critical nodes whose enhanced network segregation was related to VSOP training induced
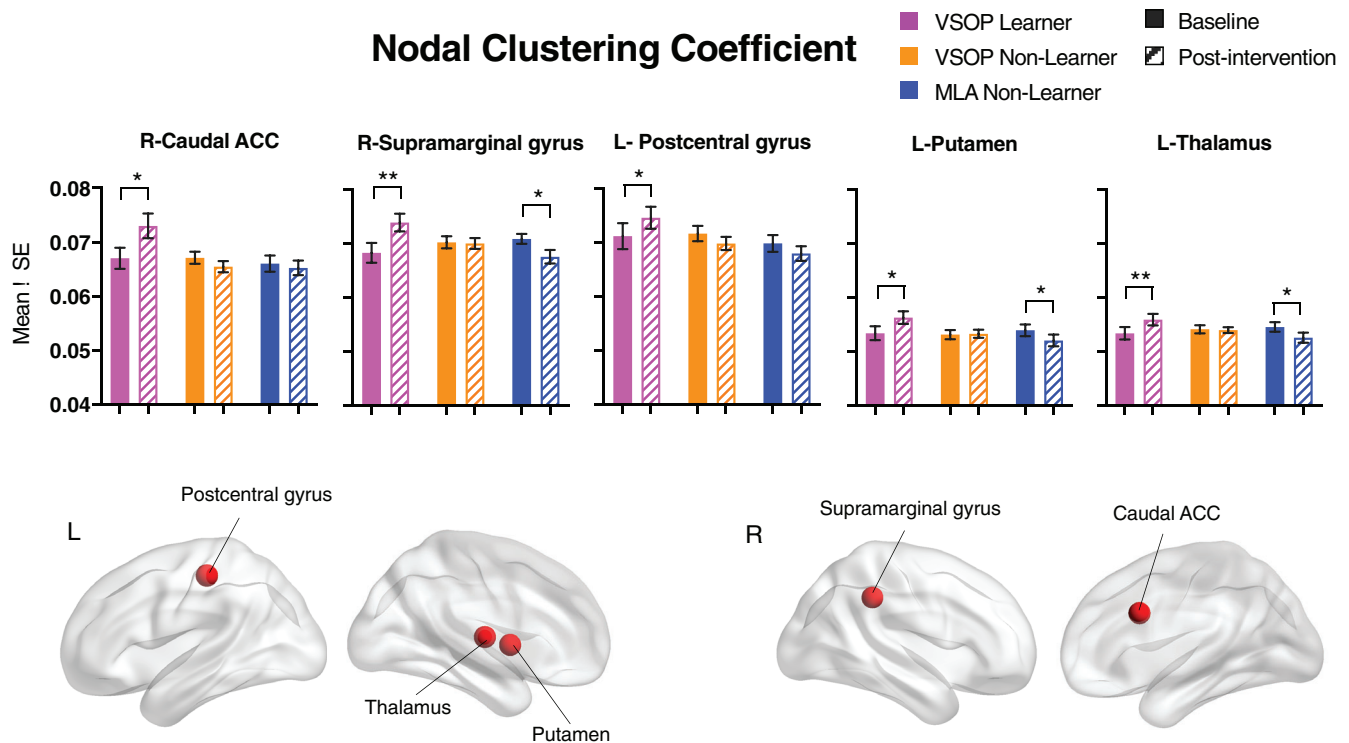
FIGURE 3 Baseline and postintervention nodal clustering coefficient for VSOP learners (pink), VSOP non-learners (orange), and MLA non-learners (blue) groups. Controlling for baseline respective nodal clustering coefficient, five regions showed significant group effect for postintervention nodal clustering coefficient after FDR correction: right caudal ACC (anterior cingulate cortex), right supramarginal gyrus, left postcentral gyrus, left putamen, and left thalamus. The five regions were visualized with the BrainNet Viewer (Xia, Wang, & He, 2013; http:// www. nitrc.org/projects/bnv/). Star represents significant within-group change from baseline to postintervention. *$p < .05$; **$p < .01$; ***$p < .001$. L, left hemisphere; R, right hemisphere

broad training effects. Also, among participants who demonstrated a broad learning effect, those with more severe baseline neurodegeneration had greater improvement in segregation after training.

These findings highlight the importance of considering whole-brain networks when attempting to understand the neural changes underlying domain general effects following training, which are essential if cognitive interventions are to improve outcomes in individuals with dementia. Changes in global network-level properties were significantly different in participants that showed this type of broad transfer, suggesting that approaches targeting these properties may be of particular benefit in future. Additionally, several specific nodes were identified as particularly important in terms of their role in the global network, potentially pointing to locations at which the network can be influenced to induce the most cognitively generalizable benefits. The fact that these changes were possible in participants with MCI is also of note: for cognitive training to be a feasible as an intervention, participants in these at-risk groups need to demonstrate the capacity to adapt following training. These results suggest that at least a subset of these individuals demonstrate sufficient network plasticity to benefit from training. Identifying what separates these participants from others at baseline may be a useful future goal for personalizing training to those that can benefit from it most.
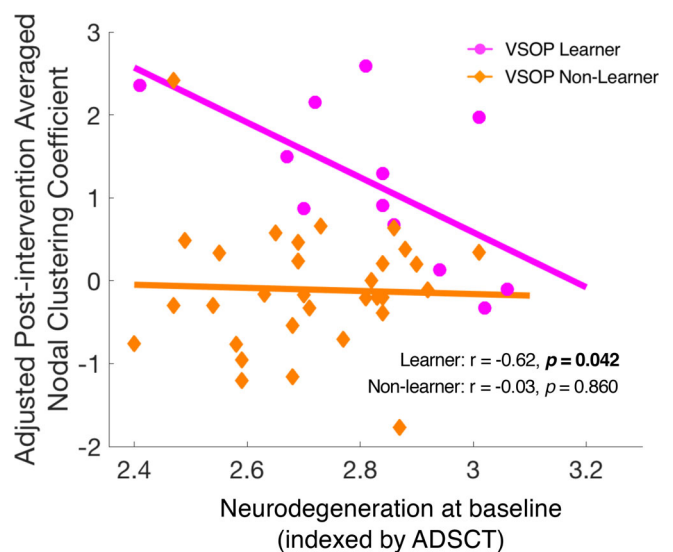

FIGURE 4 Scatterplots of baseline neurodegeneration versus neural enhancement for VSOP learner (pink) and non-learner (orange) groups. The x-axis is the baseline neurodegeneration measured by ADSCT (Alzheimer's disease signature cortical thickness). The y-axis is the postintervention averaged nodal clustering coefficient adjusted for baseline averaged nodal clustering coefficient

More specifically, our results support one of two competitive hypotheses: brain segregation, rather than integration, is related to explaining the broad training effect of VSOP training. This result is in line with those in younger adults showing that segregation plays a role in learning following cognitive training. Importantly, reduced segregation is characteristic of increasing age, and is associated with deficits in long-term episodic memory (Chan et al., 2014). Slowing or reversing this age-related decrease in segregation may therefore provide a means of attenuating memory decline as a result of brain aging. Mechanistically, this may be explained by "mismatch theory" (Lövdén et al., 2010), which emphasizes that enhancing plasticity related to practicing and modifying the efficiency of local brain clusters may be more important to inducing broad learning effects than enhancing flexibility related to coordination across multiple brain clusters. While we did not find changes in integration to play a role in broad learning, it is necessary to perform future studies using larger sample sizes that are specifically designed to identify these changes before fully excluding compensation as a potential pathway supporting the broad training effect following cognitive training (Stern et al., 2019).

While these results show that examining the whole brain as a network is essential to understanding domain general changes that may underlie broad transfer effects, several nodes in the network seem particularly important in this process. Specific local clusters included the cingulate cortex (right caudal ACC), selective parietal regions (right supramarginal gyrus and left postcentral gyrus), the striatum (putamen), and other subcortical regions (thalamus). Several studies have emphasized the critical role of the striatum in mediating transfer effects to untrained tasks after cognitive training (Dahlin et al., 2008; Dahlin, Bäckman, Neely, & Nyberg, 2009), and the thalamus is critical for regulating adaptation to environmental demands, such as those from the cognitive training, as part of the neurovisceral integration process (Mulcahy, Larsson, Garfinkel, & Critchley, 2019). Additionally, the thalamus has been shown to be integral to determining the modular organization of the brain and regulating whole-brain organization in way that allows for effective task performance (Hwang, Bertolero, Liu, & D'Esposito, 2017; Shine et al., 2019). The ability of the thalamus to modulate the overall organization of the cortex via a range of projections makes it well placed to influence cognitive function in a broad, domain general way (Behrens et al., 2003). In the cortex, the caudal ACC is a key node of the default mode network (DMN; Raichle et al., 2001), while the two parietal regions are part of the attention network (Fan, McCandliss, Fossella, Flombaum, & Posner, 2005; Vossel, Geng, & Fink, 2014). Both networks support a wide range of perceptual and cognitive abilities (Buckner, Andrews-Hanna, & Schacter, 2008; Raichle et al., 2001), with weakened connectivity underpinning a wide range of age-related cognitive decline (Andrews-Hanna et al., 2007; Geerlings et al., 2015). Additionally, the DMN has been shown to play a role in the performance of a range of tasks through flexibly coupling to other task-specific systems (Elton & Gao, 2015). Overall, these regions are well-placed to play a role in broad transfer due to their domain general role in cognitive function. Understanding exactly how the structural segregation of these nodes within the broader whole-brain network relates to their functional engagement during complex task performance is an important question going forward.

Finally, our paper showed that there was a relationship between more severe baseline brain atrophy and greater enhancement in brain segregation after training in VSOP learners but not non-learners. This observation may be particularly important when seeking for effective interventions among those with very high risk for dementia (e.g., late MCI relatively to early MCI; Aisen et al., 2010). It suggests that interventions that can enhance brain segregation may be useful in those with severe brain atrophy, who represent a particularly difficult-to-treat population at present. It will be important to test whether these effects replicate with more specific measures of Alzheimer's pathology (e.g., amyloid or tau deposition). Additionally, it will be important to understand why this relationship was only identified in learners, and what may be unique about these individuals, before global and nodal segregation can serve as biomarkers guiding the development of effective cognitive training. While developing training with these mechanisms in mind may improve outcomes for some, cognitive training alone, at least in the form of VSOP training, may not be sufficient to ensure a broad training effect for all older adults, especially those without the capacity for broad learning, whether due to more advanced neurodegeneration or yet unknown factors that determine this capacity. In participants without this natural capacity, it may be possible to facilitate brain segregation using stimulation. Transcranial direct current stimulation (tDCS) has been shown induce the enhancement of local connectivity within sensorimotor areas of the stimulated hemisphere (Polanía, Nitsche, & Paulus, 2011; Polania, Paulus, Antal, & Nitsche, 2011). Identifying regions, such as those in this study, that are particularly important to broad transfer via segregation and are amenable to surface stimulation (such as the postcentral gyrus) may enable these techniques to be combined wwith training to improve learning, particularly in hard-to-treat groups.

5 | LIMITATIONS

The major limitations of this study are its small sample size and retrospective design; thus, the findings are preliminary, providing a basis for future studies. Adequately powered randomized, controlled trials will be required to draw any firm conclusions on the neuroplasticity underlying broad training effects and their relationship to network segregation and integration. Furthermore, it is unclear whether the identified brain characteristics are specific for VSOP training or generalize to other types of cognitive training. Future studies using a greater range of training techniques will be needed to understand the specificity of these findings.

Additionally, in older adults, it is important to control for the amount of computer use, as it is possible that the novel experience of learning to use electronic devices could also lead to improvements in EM and EF. In this experiment, we included a control group in which participants completed everyday tasks such as crosswords and sudoku on the computer. The comparison between VSOP versus MLA should therefore act to exclude confounding factors including novel

computer experience (as well as training hours and practice effects more generally). However, it is possible that participants overall are more accustomed to the types of computer games in the MLA control (sudoku, crosswords, etc.) than the faster paced training game used in the VSOP group. Therefore, it is possible that some benefits seen in EM and EF could be due to the novel experience of learning to perform this type of task on the computer more generally, rather than to VSOP training specifically. It will be important in future to compare learning effects across more similar brain training tasks to understand exactly what aspect of the task might lead to these effects.

In summary, we showed that participants with MCI who showed broad transfer effects showed changes in whole-brain network properties following cognitive VSOP training, suggesting that some aging individuals at risk for dementia have the neural plasticity to show domain general improvements following targeted cognitive training. Specifically, learners showed enhanced whole-brain segregation, as well as segregation in several cortical and subcortical regions, and benefits from these changes were particularly pronounced in learners with more neurodegeneration. These regions included those in the DMN and thalamus that are known to play domain general roles in cognitive function, and this may determine their importance for broad learning. Targeting training at increasing or slowing the decline of neural segregation, particularly in these regions, may improve real-world outcomes via demonstrating domain general cognitive benefits. Understanding which people have the capacity for these changes, and whether non-learner segregation can be facilitated via neural stimulation, will be essential for further personalizing training to individuals.

ACKNOWLEDGMENT

CONFLICT OF INTEREST

The authors declare no conflict of interest.

DATA AVAILABILITY STATEMENT

PHI de-identified behavioral and imaging data will be available via IRB approval.

ORCID

Quanjing Chen https://orcid.org/0000-0003-4630-6817
Zhengwu Zhang https://orcid.org/0000-0002-9047-8838

REFERENCES

Achard, S., & Bullmore, E. (2007). Efficiency and cost of economical brain functional networks. *PLoS Computational Biology*, 3, e17.

Aisen, P. S., Petersen, R. C., Donohue, M. C., Gamst, A., Raman, R., Thomas, R. G., ... Alzheimer's Disease Neuroimaging Initiative. (2010). Clinical core of the Alzheimer's disease neuroimaging initiative: progress and plans. *Alzheimer's and Dementia*, 6, 239–246.

Albert, M. S., DeKosky, S. T., Dickson, D., Dubois, B., Feldman, H. H., & Fox, N.C. (2011). The diagnosis of mild cognitive impairment due to Alzheimer's disease: recommendations from the National Institute on Aging-Alzheimer's Association workgroups on diagnostic guidelines for Alzheimer's disease. *Alzheimer's and Dementia*, 7, 270–279.

Andrews-Hanna, J. R., Snyder, A. Z., Vincent, J. L., Lustig, C., Head, D., Raichle, M. E., & Buckner, R. L. (2007). Disruption of large-scale brain systems in advanced aging. *Neuron*, 56, 924–935.

Bamidis, P. D., Vivas, A. B., Styliadis, C., Frantzidis, C., Klados, M., Schlee, W., ... Papageorgiou, S. G. (2014). A review of physical and cognitive interventions in aging. *Neuroscience and Biobehavioral Reviews*, 44, 206–220.

Bassett, D. S., & Bullmore, E. T. (2009). Human brain networks in health and disease. *Current Opinion in Neurology*, 22, 340–347.

Behrens, T. E., Johansen-Berg, H., Woolrich, M. W., Smith, S. M., Wheeler-Kingshott, C. A. M., & Boulby, P. A. (2003). Non-invasive mapping of connections between human thalamus and cortex using diffusion imaging. *Nature Neuroscience*, 6, 750–757.

Benedict, R. H. B. (1997). *Brief visuospatial memory test: revised professional manual*. Odessa, FL: Psychological Assessment Resources, Inc.

Betzel, R. F., Byrge, L., He, Y., Goni, J., Zuo, X. N., & Sporns, O. (2014). Changes in structural and functional connectivity among resting-state networks across the human lifespan. *NeuroImage*, 102(Pt 2), 345–357.

Boccaletti, S., Latora, V., Moreno, Y., Chavez, M., & Hwang, D. (2006). Complex networks: Structure and dynamics. *Physics Reports*, 424, 175–308.

Buckner, R. L., Andrews-Hanna, J. R., & Schacter, D. L. (2008). The brain's default network: anatomy, function, and relevance to disease. *Annals of the New York Academy of Sciences*, 1124, 1–38.

Bullmore, E., & Sporns, O. (2009). Complex brain networks: graph theoretical analysis of structural and functional systems. *Nature Reviews. Neuroscience*, 10, 186–198.

Bullmore, E. T., & Bassett, D. S. (2011). Brain graphs: graphical models of the human brain connectome. *Annual Review of Clinical Psychology*, 7, 113–140.

Cao, Q., Shu, N., An, L., Wang, P., Sun, L., Xia, M. R., ... He, Y. (2013). Probabilistic diffusion tractography and graph theory analysis reveal abnormal white matter structural connectivity networks in drug-naive boys with attention deficit/hyperactivity disorder. *The Journal of Neuroscience*, 33, 10676–10687.

Cao, W., Cao, X., Hou, C., Li, T., Cheng, Y., & Jiang, L. (2016). Effects of cognitive training on resting-state functional connectivity of default mode, salience, and central executive networks. *Frontiers in Aging Neuroscience*, 8, 70.

Chan, M. Y., Park, D. C., Savalia, N. K., Petersen, S. E., & Wig, G. S. (2014). Decreased segregation of brain systems across the healthy adult lifespan. *Proceedings of the National Academy of Sciences of the United States of America*, 111, E4997–E5006.

Copay, A. G., Subach, B. R., Glassman, S. D., Polly, D. W., Jr., & Schuler, T. C. (2007). Understanding the minimum clinically important difference: a review of concepts and methods. *The Spine Journal*, 7, 541–546.

Corbetta, M. (1998). Frontoparietal cortical networks for directing attention and the eye to visual locations: identical, independent, or overlapping neural systems? *Proceedings of the National Academy of Sciences of the United States of America*, 95, 831–838.

Dahlin, E., Neely, A. S., Larsson, A., Backman, L., & Nyberg, L. (2008). Transfer of learning after updating training mediated by the striatum. *Science*, 320, 1510–1512.

Dahlin, E., Bäckman, L., Neely, A. S., & Nyberg, L. (2009). Training of the executive component of working memory: subcortical areas mediate transfer effects. *Restorative Neurology and Neuroscience*, 27, 405–419.

Dai, Z., & He, Y. (2014). Disrupted structural and functional brain connectomes in mild cognitive impairment and Alzheimer's disease. *Neuroscience Bulletin*, 30, 217–232.

Desikan, R. S., Segonne, F., Fischl, B., Quinn, B. T., Dickerson, B. C., & Blacker, D. (2006). An automated labeling system for subdividing the human cerebral cortex on MRI scans into gyral based regions of interest. *NeuroImage*, 31, 968–980.

Dudai, Y. (2004). *Memory from A to Z. Keywords, Concepts, and Beyond.* Oxford, England: Oxford University Press.

Elton, A., & Gao, W. (2015). Task-positive functional connectivity of the default mode network transcends task domain. *Journal of Cognitive Neuroscience, 27*, 2369–2381.

Fan, J., McCandliss, B. D., Fossella, J., Flombaum, J. I., & Posner, M. I. (2005). The activation of attentional networks. *NeuroImage, 26*, 471–479.

Fissler, P., Muller, H. P., Kuster, O. C., Laptinskaya, D., Thurm, F., & Woll, A. (2017). No evidence that short-term cognitive or physical training programs or lifestyles are related to changes in white matter integrity in older adults at risk of dementia. *Frontiers in Human Neuroscience, 11*, 110.

Geerligs, L., Renken, R. J., Saliasi, E., Maurits, N. M., & Lorist, M. M. (2015). A brain-wide study of age-related changes in functional connectivity. *Cerebral Cortex, 25*, 1987–1999.

Girard, G., Whittingstall, K., Deriche, R., & Descoteaux, M. (2014). Towards quantitative connectivity analysis: reducing tractography biases. *NeuroImage, 98*, 266–278.

Goldman-Rakic, P. S. (1988). Topography of cognition: parallel distributed networks in primate association cortex. *Annual Review of Neuroscience, 11*, 137–156.

Gong, G., He, Y., Concha, L., Lebel, C., Gross, D. W., Evans, A. C., & Beaulieu, C. (2009). Mapping anatomical connectivity patterns of human cerebral cortex using in vivo diffusion tensor imaging tractography. *Cerebral Cortex, 19*, 524–536.

He, Y., Chen, Z., & Evans, A. (2008). Structural insights into aberrant topological patterns of large-scale cortical networks in Alzheimer's disease. *The Journal of Neuroscience, 28*, 4756–4766.

Humphries, M. D., & Gurney, K. (2008). Network 'small-world-ness': a quantitative method for determining canonical network equivalence. *PLoS One, 3*, e0002051.

Hwang, K., Bertolero, M. A., Liu, W. B., & D'Esposito, M. (2017). The human thalamus is an integrative hub for functional brain networks. *The Journal of Neuroscience, 37*, 5594–5607.

Jack, C. R., Jr., Wiste, H. J., Weigand, S. D., Knopman, D. S., Mielke, M. M., Vemuri, P., ... Petersen, R. C. (2015). Different definitions of neurodegeneration produce similar amyloid/neurodegeneration biomarker group findings. *Brain, 138*, 3747–3759.

Koen, J. D., & Rugg, M. D. (2019). Neural dedifferentiation in the aging brain. *Trends in Cognitive Sciences, 23*, 547–559.

Kramer, J. H., Mungas, D., Possin, K. L., Rankin, K. P., Boxer, A. L., Rosen, H. J., ... Widmeyer, M. (2014). NIH EXAMINER: conceptualization and development of an executive function battery. *Journal of the International Neuropsychological Society, 20*, 11–19.

Kraus, M. F., Susmaras, T., Caughlin, B. P., Walker, C. J., Sweeney, J. A., & Little, D. M. (2007). White matter integrity and cognition in chronic traumatic brain injury: a diffusion tensor imaging study. *Brain, 130*, 2508–2519.

Lampit, A., Hallock, H., & Valenzuela, M. (2014). Computerized cognitive training in cognitively healthy older adults: a systematic review and meta-analysis of effect modifiers. *PLoS Medicine, 11*, e1001756.

Langer, N., von Bastian, C. C., Wirz, H., Oberauer, K., & Jancke, L. (2013). The effects of working memory training on functional brain network efficiency. *Cortex, 49*, 2424–2438.

Liang, P., Wang, Z., Yang, Y., Jia, X., & Li, K. (2011). Functional disconnection and compensation in mild cognitive impairment: evidence from DLPFC connectivity using resting-state fMRI. *PLoS One, 6*, e22153.

Lin, F., Ren, P., Wang, X., Anthony, M., Tadin, D., & Heffner, K. L. (2017). Cortical thickness is associated with altered autonomic function in cognitively impaired and non-impaired older adults. *The Journal of Physiology, 595*, 6969–6978.

Lin, F. V., Tao, Y., Chen, Q., Anthony, M., Zhang, Z., Tadin, D., & Heffner, K. L. (2020). Processing speed and attention training modifies

autonomic flexibility: A mechanistic intervention study. *NeuroImage, 213*, 116730.

Lövdén, M., Backman, L., Lindenberger, U., Schaefer, S., & Schmiedek, F. (2010). A theoretical framework for the study of adult cognitive plasticity. *Psychological Bulletin, 136*, 659–676.

Meunier, D., Lambiotte, R., Fornito, A., Ersche, K. D., & Bullmore, E. T. (2009). Hierarchical modularity in human brain functional networks. *Frontiers in Neuroinformatics, 3*, 37.

Miraglia, F., Vecchio, F., & Rossini, P. M. (2018). Brain electroencephalographic segregation as a biomarker of learning. *Neural Networks, 106*, 168–174.

Mulcahy, J. S., Larsson, D. E. O., Garfinkel, S. N., & Critchley, H. D. (2019). Heart rate variability as a biomarker in health and affective disorders: A perspective on neuroimaging studies. *NeuroImage, 202*, 116072.

Onoda, K., & Yamaguchi, S. (2013). Small-worldness and modularity of the resting-state functional brain network decrease with aging. *Neuroscience Letters, 556*, 104–108.

Park, D. C., & Reuter-Lorenz, P. (2009). The adaptive brain: aging and neurocognitive scaffolding. *Annual Review of Psychology, 60*, 173–196.

Park, H. J., Kubicki, M., Westin, C. F., Talos, I. F., Brun, A., Peiper, S., ... Shenton, M. E. (2004). Method for combining information from white matter fiber tracking and gray matter parcellation. *American Journal of Neuroradiology, 25*, 1318–1324.

Polanía, R., Nitsche, M. A., & Paulus, W. (2011). Modulating functional connectivity patterns and topological functional organization of the human brain with transcranial direct current stimulation. *Human Brain Mapping, 32*, 1236–1249.

Polania, R., Paulus, W., Antal, A., & Nitsche, M. A. (2011). Introducing graph theory to track for neuroplastic alterations in the resting human brain: a transcranial direct current stimulation study. *NeuroImage, 54*, 2287–2296.

Raichle, M. E., MacLeod, A. M., Snyder, A. Z., Powers, W. J., Gusnard, D. A., & Shulman, G. L. (2001). A default mode of brain function. *Proceedings of the National Academy of Sciences United States of America, 98*, 676–682.

Rossetti, H. C., Lacritz, L. H., Cullum, C. M., & Weiner, M. F. (2011). Normative data for the Montreal Cognitive Assessment (MoCA) in a population-based sample. *Neurology, 77*, 1272–1275.

Rubinov, M., & Sporns, O. (2010). Complex network measures of brain connectivity: Uses and interpretations. *NeuroImage, 52*, 1059–1069.

Salthouse, T. A. (1996). The processing-speed theory of adult age differences in cognition. *Psychological Review, 103*, 403–428.

Shao, Y. K., Mang, J., Li, P. L., Wang, J., Deng, T., & Xu, Z. X. (2015). Computer-based cognitive programs for improvement of memory, processing speed and executive function during age-related cognitive decline: A meta-analysis. *PLoS One, 10*, e0130831.

Shine, J. M., Hearne, L. J., Breakspear, M., Hwang, K., Muller, E. J., & Sporns, O. (2019). The low-dimensional neural architecture of cognitive complexity is related to activity in medial thalamic nuclei. *Neuron, 104*, 849–55 e3.

Smith, S. M. (2002). Fast robust automated brain extraction. *Human Brain Mapping, 17*, 143–155.

Song, J., Birn, R. M., Boly, M., Meier, T. B., Nair, V. A., Meyerand, M. E., & Prabhakaran, V. (2014). Age-related reorganizational changes in modularity and functional connectivity of human brain networks. *Brain Connectivity, 4*, 662–676.

Stern, Y., Chetelat, G., Habeck, C., Arenaza-Urquijo, E. M., Vemuri, P., & Estanga, A. (2019). Mechanisms underlying resilience in ageing. *Nature Reviews. Neuroscience, 20*, 246.

Takeuchi, H., Sekiguchi, A., Taki, Y., Yokoyama, S., Yomogida, Y., Komuro, N., ... Kawashima, R. (2010). Training of working memory impacts structural connectivity. *The Journal of Neuroscience, 30*, 3297–3303.

Taya, F., Sun, Y., Babiloni, F., Thakor, N., & Bezerianos, A. (2015). Brain enhancement through cognitive training: a new insight from brain connectome. *Frontiers in Systems Neuroscience*, 9, 44.

Thayer, J. F., Hansen, A. L., Saus-Rose, E., & Johnsen, B. H. (2009). Heart rate variability, prefrontal neural function, and cognitive performance: the neurovisceral integration perspective on self-regulation, adaptation, and health. *Annals of Behavioral Medicine*, 37, 141–153.

Vossel, S., Geng, J. J., & Fink, G. R. (2014). Dorsal and ventral attention systems: distinct neural circuits but collaborative roles. *The Neuroscientist*, 20, 150–159.

Wang, J., Wang, X., Xia, M., Liao, X., Evans, A., & He, Y. (2015). GRETNA: a graph theoretical network analysis toolbox for imaging connectomics. *Frontiers in Human Neuroscience*, 9, 386.

Watts, D., & Strogatz, S. (1998). Collective dynamics of "small-world" networks. *Nature*, 393, 440–442.

Woutersen, K., Guadron, L., van den Berg, A. V., Boonstra, F. N., Theelen, T., & Goossens, J. (2017). A meta-analysis of perceptual and cognitive functions involved in useful-field-of-view test performance. *Journal of Vision*, 17, 11.

Xia, M., Wang, J., & He, Y. (2013). BrainNet Viewer: a network visualization tool for human brain connectomics. *PLoS One*, 8, e68910.

Yuan, J. P., Henje Blom, E., Flynn, T., Chen, Y., Ho, T. C., Connolly, C. G., ... Tymofiyeva, O. (2019). Test: retest reliability of graph theoretic metrics in adolescent brains. *Brain Connectivity*, 9, 144–154.

Zhang, Z., Descoteaux, M., Zhang, J., Girard, G., Chamberland, M., Dunson, D., ... Zhu, H. (2018). Mapping population-based structural connectomes. *NeuroImage*, 172, 130–145.

SUPPORTING INFORMATION

Additional supporting information may be found online in the Supporting Information section at the end of this article.

How to cite this article: Chen Q, Baran TM, Turnbull A, Zhang Z, Rebok GW, Lin FV. Increased segregation of structural brain networks underpins enhanced broad cognitive abilities of cognitive training. *Hum Brain Mapp*. 2021;42: 3202–3215. https://doi.org/10.1002/hbm.25428